Analytical Truss Models for Prediction the Shear Strength of FRP Strengthened Reinforced Concrete Members

W. Teo[1], Y. Hor[2]
[1]Senior Lecturer, Universiti Teknologi PETRONAS, Malaysia, wee.teo@gmail.com
[2]MSc Candidate, Universiti Teknologi PETRONAS, Malaysia

Keywords: Reinforced concrete; Debonding; Shear failure; CFRP; Shear strengthening; Beam.

SUMMARY
This paper presents an optimised truss model based on the principle of minimum total strain energy theorem. The validation of the model was done through 24 experimental test results found in the literature. The results obtained showed that the optimised truss model with effective strain from ACI 440 derived the most viable model, with average shear strength ratio and COV of 0.99 and 20% respectively. This model also demonstrated its capability to truly capture the actual behaviour and failure modes. It is also interesting to note that the optimised truss model tends to yield better prediction in 2-sides bonded (2S) than in U-wrap (U). Overall, the results obtained from this analysis were very encouraging. It is suggested that more validation are still needed to confirm the suitability of this model.

1. INTRODUCTION

Considerable research had been conducted on FRP shear strengthening, justifying their application and reliability without questions. The problem with shear failure of a reinforced concrete (RC) beam strengthened with FRP is a complex and controversial subject even for simple RC beams and is still remains not fully understood. Over the years, many analytical models and design equations have been developed for RC beams strengthened with FRP. Despite that, there still lacks agreement in term of their prediction and accuracy.

Current design procedure for FRP strengthened members is based entirely on 45-deg truss analogy. Although this approach is simple and well known for overestimating the shear strength of the members, it does not provide correct representation to the actual stress distribution. An optimised truss model based on the principle of minimum strain energy is proposed in this paper. One distinguishing difference with standard truss model is that the compression struts are not imposed to be parallel at 45-deg, instead it varies along the shear span. To develop a realistic model, the optimised model was characterised by various limiting failure criteria. One in particular is the FRP laminate debonding failure mode which is common for externally-bonded composite strengthened members. The FRP contribution to shear resistance is limited by the effective strain of FRP ($\varepsilon_{frp,e}$). In recent years, many researchers have proposed various formulations to calculate $\varepsilon_{frp,e}$.

The determination of an acceptable $\varepsilon_{frp,e}$ formulation to be used in the proposed analytical model is desirable. This paper presents the results of the analysis carried out by five commonly and recently developed $\varepsilon_{frp,e}$ formulations in our optimised truss model. Their respective accuracy in predicting the FRP shear contribution as well as modes of failure was evaluated. Viability of the model is done through validation against a set of experiment database collected from the existing literatures. In the

initial part of this paper, details on the features and procedures involved in the development of optimised truss model will be discussed.

2. EXPERIMENT DATABASE DESCRIPTION

In this paper, an experiment database representing 24 RC beams externally strengthened in shear with only FRP laminate strip systems were collected from published literatures [9-16]. These can be divided into two groups: (a) 2-sides bonded (2S) and (b) 3-sides bonded or sometimes known as U-wrap (U). Figure 1 shows the externally bonded FRP strengthening schemes adopted. 17 beams were provided with 2-sides bonded, and 7 beams with U-wrap. Out of the 24 beams, six were orientated at an angle of 45-deg and only one beam was orientated at 25-deg. All beams were strengthened externally with FRP and without any internal shear reinforcement, in order to investigate purely the FRP shear contribution. The type of fibre used in all the beams was carbon. Details of the geometrical and material properties of the beam specimens are summarised in Tables 1 and 2, which may be downloaded online from the following URL link: (https://docs.google.com/folder/d/0B_MFOj1n50n6VzgzaUIwYk5Dbk0/edit).

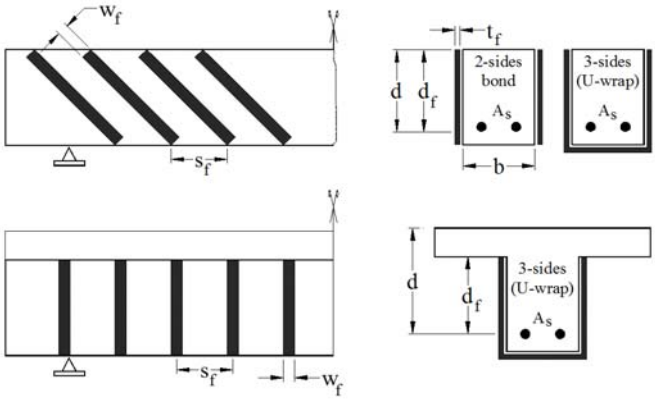

Figure 1: FRP strengthening schemes

3. ANALYTICAL TRUSS MODEL FOR FRP SHEAR CONTRIBUTION

In current code provisions [1-2] on externally bonded FRP system, the nominal shear strength V_n of the strengthened members were usually calculated as the summation of the concrete (V_c), shear steel (V_s) and FRP (V_{frp}) contributions, as follows:

$$V_n = V_c + V_s + V_{frp} \tag{1}$$

In this study, similar formulation was adopted to calculate the shear strength capacity of FRP strengthened members. The shear strength of the concrete V_c may be calculated according to the shear design provisions in the current codes (such as ACI 318-08 [3]) which is based entirely on semi-empirical expression. But since the shear topic still remains controversial, to avoid any disagreement and maintain consistency throughout, the V_c value adopted in this study is based on the actual test value obtained directly from experiment control specimens. As for the V_s contribution, it was omitted because the beam specimens considered in this study were specially selected without including the internal shear reinforcement, as explained in the preceding section.

3.1 Evaluation of FRP Shear Contribution

In this study, the V_{frp} contribution was computed based on the Strut-and-Tie Model (STM) approach. The STM is basically a generalisation of the truss analogy originally proposed by Ritter [4] and Mörsch [5] in the early of last century. STM had long been recognised as the rational conceptual tool for design and detailing of RC members. This research is intended to extend the application of STM to

externally bonded CFRP shear strengthened beams. An optimal STM model that corresponded well with the actual stress fields was proposed for FRP strengthened beams. The overall computational process to derive V_{frp} and failure modes from this optimal model may be divided into two parts, namely:
(a) Part A for truss model optimisation,
(b) Part B to evaluate the limiting strength of the optimised truss model.

Figure 2 summarises the overall procedure of the computational process. In the following sections, each part of the computational process will be discussed in more details.

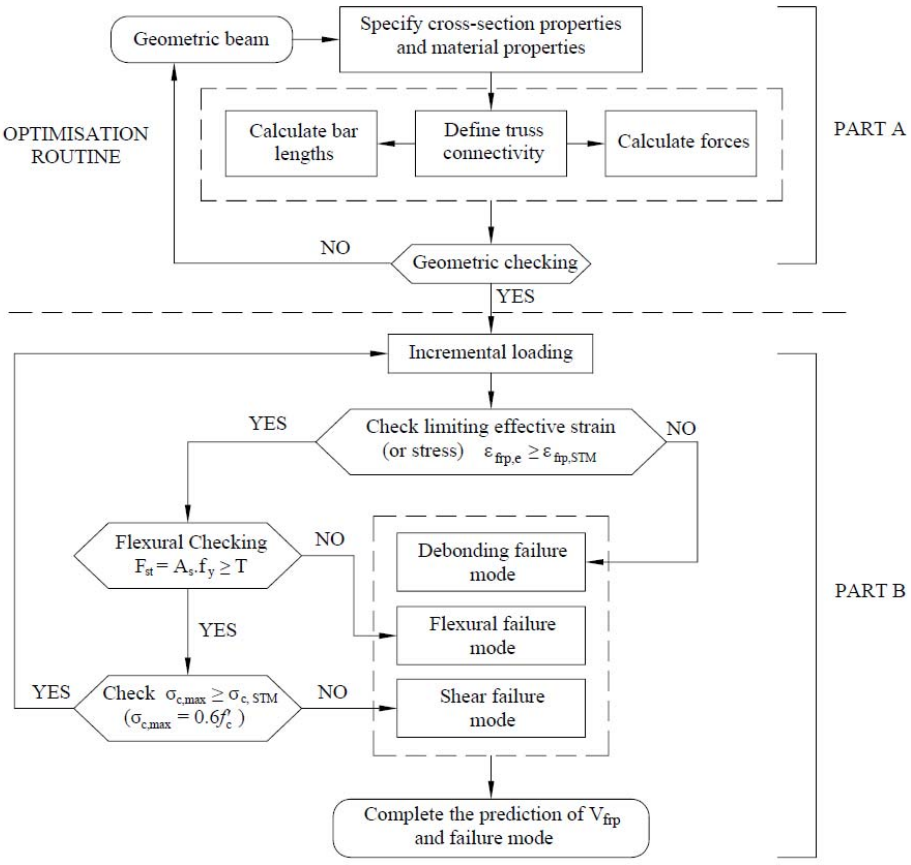

Figure 2: Procedures for evaluation of V_{frp} and modes of failure.

3.1.1 Truss Model Optimisation (Part A)

The internal stress distribution of FRP strengthened members was visualised by STM through two main resultant elements; namely compression struts and tensile ties. The compression struts represent the concrete stress fields with compression in the direction of the strut. As for the tensile ties, it represents two components: (1) internal longitudinal reinforcement and (2) external FRP systems. Figure 3 shows the proposed outline of the STM models used in this study.

To begin with the truss geometry, the first step is to define the lever arm (Z value showed in Figure 3) of the beam cross-section. A fixed value of 0.8d was adopted in this study. This Z value helps to define the top and bottom chords of the truss. After that, the tensile ties along the shear span may be positioned according to the FRP configuration and longitudinal reinforcement. Once it had been done, the compression struts can then be outlined.

To develop a suitable model that could represent the actual internal stress fields of an RC structure is a tedious and iterative process. With so many possible models, doubts could arise as to whether the correct model has been chosen. In mechanics theory, it had long been recognised that loads are transmitted based on the principle of minimum strain energy. In this study, the optimisation formulation suggested by Schlaich et al [6] that based on this principle was employed. The objective function for minimising total strain energy may be written as follows:

$$MINIMUM \quad E_{pot}(\alpha_i) = \sum_{i=1}^{N} F_i l_i \varepsilon_i \tag{2}$$

where E_{pot} is the total strain energy of a beam, F_i is the tensile force in tie member i (included both internal longitudinal reinforcement and external FRP system), l_i is the length of tie member i, ε_i is the strain of tie member i and α_i is the angle of inclination of the concrete struts member i.

It can be seen that the value of E_{pot} is dependent greatly on the angle α. Therefore this angle constitutes the main variable to be determined in the analysis and to define the final outline of the compression struts. It is interesting to note that only tensile tie members was included in the computation owing to the reason that the longitudinal reinforcement steel ties are usually much more deformable (larger strains) than the concrete struts.

The final resulting optimised truss models obtained from the analysis are illustrated in Figure 3(a)-(c). Two outlines of models were presented in the figure that corresponded to two a/d ratios: (1) a/d ≤ 2.5 and (2) a/d > 2.5. It can be seen that the proposed outlines of the models more closely represent the actual stress distribution of the beams, whereby the compression struts are not imposed to be parallel at standard 45-deg throughout instead varies along the shear span.

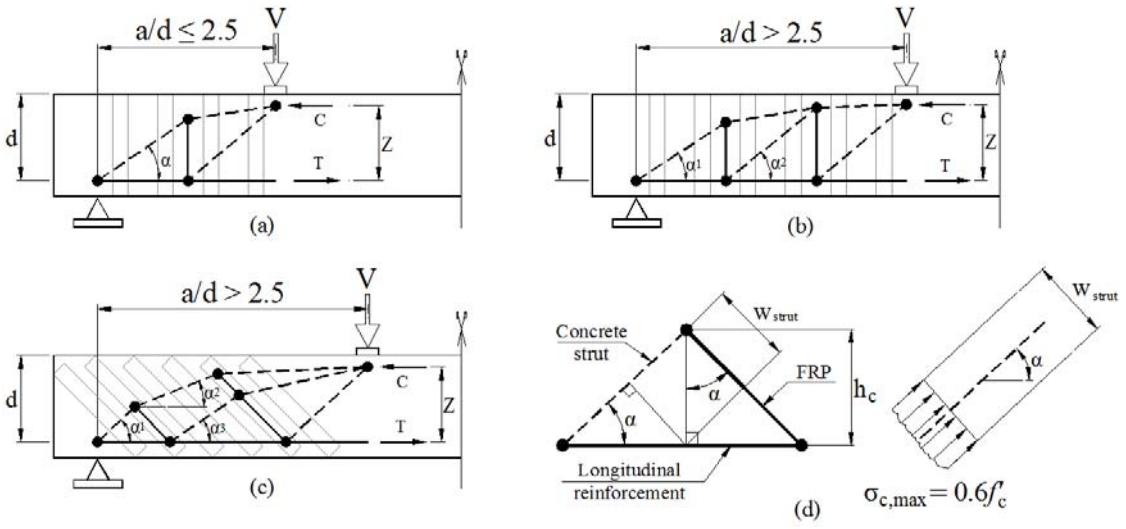

Figure 3: Strut-and-tie model for FRP strengthened beams with (a) a/d ≤ 2.5 with vertical FRP strips, (b) a/d > 2.5 with vertical FRP strips, (c) a/d > 2.5 with inclined FRP strips, and (d) Dimensioning of the width of concrete strut.

3.1.2 Limiting Strength of the Optimised Models (Part B)

Once the optimised model had been defined, it was then subjected to incremental loading to assess the limiting strength of the model, see Figure 2. To characterise and develop a realistic model, limiting failure criteria that corresponded to different type of possible failure modes undergone by FRP strengthened members was considered inside the models. Generally, there are three types of failure modes: (a) Flexural failure, (b) Strut failure (diagonal shear failure), and (c) De-bonding failure.

Flexural failure was characterised by yielding of longitudinal reinforcement. All beams considered in the analysis were under-reinforced and stress redistribution due to cracking was considered by setting an upper limit on lever arm Z as 0.8d, as explained in the preceding section. The allowable tensile capacity Fst due to yielding of steel is taken as:

$$F_{st} = A_s f_y \geq T \tag{3}$$

where f_y is the yield strength of steel, A_s is the amount of longitudinal reinforcement and T represent the tensile force applied at the tension zone due to external couple moment. Flexural failure is considered to take place when T exceeds the allowance F_{st}.

The effective strength of diagonal concrete struts $\sigma_{c,\,max}$ is often expressed as a fraction of the uniaxial concrete compressive strength f'_c:

$$\sigma_{c,max} = \nu f'_c \tag{4}$$

where ν is an effectiveness factor to account for the softening of concrete strut due to cracking and transverse tensile strains. According to Marti [19], the effective strength of concrete strut may be reasonably taken as $0.6f'_c$. Concrete strut failure or diagonal shear failure is considered to occur when the strut stress $\sigma_{c,STM}$ calculated from STM (equation (5)) exceed the effective strength $\sigma_{c,\,max}$ (equation (4)). The strut stress $\sigma_{c,STM}$ is

$$\sigma_{c,STM} = \frac{C_{strut}}{w_{strut} \cdot b} \qquad and \qquad w_{strut} = h_c Cos\alpha \tag{5}$$

where C_{strut} is the strut force calculated from STM, w_{strut} is the effective strut width, h_c is the vertical projection of a concrete strut between two nodes (see Figure 2(d)) and α is the angle inclination of concrete strut. The dimensioning of the effective strut width was illustrated in Figure 2(d).

Shear failure of strengthened beams with laminate strips were often characterised by FRP debonding failure mode [7, 8, 10]. The debonding failure was taken into account in the model by means of limiting the maximum calculated stress in the FRP from STM ($\varepsilon_{frp,STM}$) with an effective FRP strain (or stress) values ($\varepsilon_{frp,e}$). Once $\varepsilon_{frp,STM}$ exceed $\varepsilon_{frp,e}$, then FRP laminates were considered to debond. The $\varepsilon_{frp,STM}$ is calculated as:

$$\varepsilon_{frp,STM} = \frac{f_{frp,STM}}{E_{frp}} \quad where: \; f_{frp,STM} = \frac{T_{tie}}{A_{frp}} \tag{6}$$

T_{tie} is the FRP tensile tie forces calculated from STM, A_{frp} is the cross-section area of FRP strips/sheets and E_{frp} is the elastic modulus of FRP. The effective strain ($\varepsilon_{frp,e}$) have been the subject of discussions for many years and various formulations were proposed. With so many proposed formulations, doubts could arise as to which $\varepsilon_{frp,e}$ approach produces the most accurate prediction. As part of this study, the $\varepsilon_{frp,e}$ proposed by various sources [1, 2, 7, 8, 10] were evaluated through implementation in proposed optimised truss model. In the following section, the selected $\varepsilon_{frp,e}$ models used in the analysis will be presented.

3.2 Limiting Effective FRP Strain

As mentioned in preceding section, the effective strains $\varepsilon_{frp,e}$ taken from various sources were implemented in the optimised truss model in order to assess their accuracy in predicting the FRP shear contribution (V_{frp}). Five most commonly cited $\varepsilon_{frp,e}$ models were selected in this study, they are:

ACI440 [1], fib Bulletin 14 [2], Chen et al. [7], Bukhari et al. [8] and Zhang et al. [10]. Summary of each formulation are shown in Table 3.

Table 3: Effective strain models for FRP debonding

Models	***Expressions of effective strain (or stress) calculation***
ACI440.2R-08 [1]	$\varepsilon_{fe} = \kappa_\upsilon . \varepsilon_{fu} \le 0.004$; $\kappa_\upsilon = \dfrac{\kappa_1 . \kappa_2 . L_e}{11900 . \varepsilon_{fu}}$; $\kappa_\upsilon \le 0.75$ $L_e = \dfrac{23300}{\left(n_f . t_f . E_f\right)^{0.58}}$; $\kappa_1 = \left(\dfrac{f'_c}{27}\right)^{2/3}$; $\kappa_2 = \begin{cases} \dfrac{d_{fv} - 2L_e}{d_{fv}} & ; \ 2\,sides - bond \\ \dfrac{d_{fv} - L_e}{d_{fv}} & ; \ U - wraps \end{cases}$
fib Bulletin 14 [2] Note: f_{cm} and E_f are in MPa and GPa respectively.	$\varepsilon_{fe,\kappa} = \kappa \cdot \varepsilon_{fe}$; $\kappa = 0.8$ $\varepsilon_{fe} = \min\left\{ \underbrace{\left(0.65 \cdot \left(\dfrac{{f_{cm}}^{2/3}}{E_f \cdot \rho_f / 1000} \right) \right)^{0.56} \times 10^{-3}}_{CFRP\ peeling\ off\ failure} , \underbrace{0.17 \cdot \left(\dfrac{{f_{cm}}^{2/3}}{E_f \cdot \rho_f / 1000} \right)^{0.30} \cdot \varepsilon_{fu}}_{CFRP\ fracture\ failure} \right\}$
Chen and Teng [7]	$f_{frp,e} = D_{frp} \sigma_{frp,\max}$ $D_{frp} = \begin{cases} \dfrac{2}{\pi\lambda} \dfrac{1 - \cos\frac{\pi}{2}\lambda}{\sin\frac{\pi}{2}\lambda} & if \quad \lambda \le 1 \\ 1 - \dfrac{\pi - 2}{\pi\lambda} & if \quad \lambda > 1 \end{cases}$; $\sigma_{frp,\max} = \min\begin{cases} f_{frp} \\ 0.427 \beta_w \beta_L \sqrt{\dfrac{E_{frp}\sqrt{f'_c}}{t_{frp}}} \end{cases}$ $\lambda = \dfrac{L_{\max}}{L_e}$; $L_e = \sqrt{\dfrac{E_{frp} t_{frp}}{\sqrt{f'_c}}}$; $L_{\max} = \begin{cases} \dfrac{h_{frp,e}}{\sin\beta} & for\ U\ jackets \\ \dfrac{h_{frp,e}}{2\sin\beta} & for\ side\ plates \end{cases}$ $\beta_L = \begin{cases} 1 & if\ \lambda \ge 1 \\ \sin\dfrac{\pi\lambda}{2} & if\ \lambda < 1 \end{cases}$; $\beta_w = \sqrt{\dfrac{2 - \frac{w_{frp}}{s_{frp}\sin\beta}}{1 + \frac{w_{frp}}{s_{frp}\sin\beta}}}$
Zhang and Hsu [10]	$\varepsilon_{fe} = R \cdot \varepsilon_{fu}$ $R = \min\left(1.4871 \cdot \left(\dfrac{\rho_f \cdot E_f}{f'_c} \right)^{-0.7488} , \dfrac{\tau_{\max} \cdot L_e}{2 \cdot f_{fu} \cdot t_f} \right)$ $\dfrac{\tau_{\max} \cdot L_e}{2 \cdot f_{fu} \cdot t_f} \le 1$; $L_e = 75mm$; $\tau_{\max} = \left(7.64 \cdot 10^{-4} \cdot {f'_c}^2\right) - \left(2.73 \cdot 10^{-2} \cdot f'_c\right) + 6.38$
Bukhari et al. [8]	$\varepsilon_{fe} = 0.7 \cdot \left(40.25 \cdot \left(\rho_f E_f / {f'_c}^{2/3} \right)^{-0.70} \right) \times 10^{-3} \le 0.4 \cdot \varepsilon_{fu} \le 0.004$ *for side wrap* $\varepsilon_{fe} = 0.8 \cdot \left(29.14 \cdot \left(\rho_f E_f / {f'_c}^{2/3} \right)^{-0.48} \right) \times 10^{-3} \le 0.4 \cdot \varepsilon_{fu} \le 0.004$ *for U wrap*

4. VALIDATION OF THE ANALYTICAL TRUSS MODEL

To verify the accuracy of the optimised truss model, the results of the analysis was illustrated in the form of shear strength ratio ($V_{n,exp}/V_{n,STM}$) in Table 4 and graphically in Figure 4. The shear strength ratio is calculated as the ratio of the ultimate shear strength of FRP strengthened beams obtained from experiment ($V_{n,exp}$) to ultimate shear strength predicted from STM ($V_{n,STM}$), whereby the $V_{n,STM}$ may be computed as the summation of ultimate shear strength from control test beams ($V_{c,exp}$) and predicted FRP shear contribution from STM ($V_{frp,STM}$), refer to Table 4 for more details.

Generally, it is evident that the shear strength prediction by optimised truss model performed reasonably well. Most of the effective strain formulations (fib Bulletin 14, Chen et al., Zhang et al. and Bukhari et al.) resulted an overestimate of shear strength with average $V_{n,exp}/V_{n,STM}$ ratio in the range between 0.81 – 0.85 and coefficient of variation (COV) between 24.1% – 29.3%, see Table 4 and Figure 4. Of all, the effective strain formulation from ACI 440 [1] gave the most accuracy prediction for shear strength with $V_{n,exp}/V_{n,STM}$ ratio and COV of 0.99 and 20% respectively. The effective strain of ACI 440 provision is calculated based on the FRP-concrete bond mechanism suggested by Khalifa et al. [18].

The effect of different strengthening schemes on the accuracy of this optimised model are summarised in Table 5. As mentioned previously in section 2, out of the 24 beams, 17 of them were 2-sides bonded (2S) and 7 of them were U-wrap (U). It can be seen that the performance of ACI 440 effective strain still remain satisfactory. Under 2-sides bonded, the average $V_{n,exp}/V_{n,STM}$ ratio and COV obtained were 1.02 and 18.6% respectively. As a matter of fact, ACI 440 gave the best prediction compared with other formulations. As for U-wrap, their performance was moderate. The average $V_{n,exp}/V_{n,STM}$ ratio and COV obtained were 0.92 and 24.1% respectively. Figure 4(a) showed that both strengthening schemes are very well distributed around the bisector line, which indicated that ACI effective strain formulation is an acceptable approach to derive a viable model.

Besides shear strength, the optimised models are also used to predict the modes of failure observed from the experiment. The results of the predictions are summarised in Table 6. It can be seen that in comparison with experiment observation, the optimised truss model with effective strains from ACI 440 predicted very closely to the actual modes of failure exhibited, except for those specimens from Triantafillou [14]. Of all five formulations, the worst is from *fib*. The *fib* formulations are based entirely on the regression of experimental results carried out by Triantafillou and Antonopoulos [15]. Due to its empirical nature based on limited database, its prediction accuracy is without doubt unsatisfactory.

So far based on current experiment database (24 specimens); the results obtained showed very promising. As a whole, it had shown that the optimised truss model with ACI effective strain formulation derived the most viable model whereby it produced the most accurate prediction and realistic representation on the behaviour of FRP strengthened members. However, more databases are still needed to further verify the reliability and accuracy of this optimised model.

5. CONCLUSIONS AND RECOMMENDATIONS

An optimised truss model based on the principle of minimum total strain energy for the evaluation of RC beams strengthened in shear with FRP was presented. To develop a realistic model, the proposed model was characterised by various limiting failure criteria. One in particular is the FRP debonding failure mode. An assessment into the effective FRP strain formulations proposed by various researchers was carried out. From this study, the following conclusions can be drawn:

(a) Based on the collected experiment database from published literatures, the optimised model with effective strain formulation from ACI 440 produced the most accurate prediction of shear strength

with average $V_{n,exp}/V_{n,STM}$ ratio and COV of 0.99 and 20% respectively. Figure 4(a) showed that the datasets are very well distributed around the bisector line based on ACI effective strain. Other formulations (*fib* Bulletin 14, Chen et al., Zhang et al. and Bukhari et al.) also showed satisfactory results, but overestimated the shear strength (see Figure 4(b)-(e)).

(b) Regardless of which effective strain formulations, the optimised model tends to produce better prediction in 2-sides bonded (2S) than in U-wrap (U). More research is still needed to improve the accuracy of U-wrap prediction using this model. For both strengthening schemes, ACI effective strain still gave the best prediction, see Table 5.

(c) The capability of this optimised model to predict the modes of failure observed from experiment was demonstrated. The best prediction was again with effective strain from ACI 440, whereby it was able to truly capture the actual failure behaviour. The worst prediction was however from *fib*.

(d) As a conclusion, this study showed that the optimised truss model with ACI effective strain formulation derived the most viable model. However, more databases are still needed to verify the reliability and accuracy of this model.

Table 4: Comparison between experimental and STM prediction on the shear strength of FRP strengthened beams

Reference	***Beam No***	***Experimental***		***Ratio of $V_{n,exp}/V_{n,STM}$ based on***				
		$V_{n,exp}$ (kN)	***$V_{c,exp}$ (kN)***	***ACI[1]***	***fib[2]***	***Chen[3]***	***Zhang[4]***	***Buk[5]***
Teo et al. [9]	A2	58.0	31.8	0.84	0.61	0.80	0.57	0.77
	A3	63.0	31.8	1.08	0.82	0.88	0.77	1.00
	A4	68.2	31.8	1.31	1.08	0.91	0.99	1.30
Zhang et al. [10]	Z4-90	73.7	46.1	0.84	0.77	0.77	0.77	0.77
	Z4-45	82.8	46.1	1.06	0.87	0.88	0.90	0.90
	Z6-90	63.9	43.0	0.75	0.69	0.69	0.69	0.69
	Z6-45	55.6	42.5	0.87	0.67	0.74	0.76	0.76
Barros et al. [11]	A10-M	61.0	50.2	0.85	0.59	0.59	0.80	0.59
	B10-M	55.6	37.0	0.75	0.65	0.59	0.71	0.65
	A12-M	89.8	58.3	0.79	0.59	0.66	0.73	0.59
	B12-M	71.5	37.9	0.64	0.58	0.63	0.61	0.58
Kim et al. [12]	CP2-1VS	163.0	105.0	0.98	0.64	0.82	0.72	0.69
	CP2-1DS	178.0	105.0	1.12	0.81	0.89	0.83	0.91
	CP3-1VS	94.5	62.5	0.84	0.53	0.68	0.58	0.55
Mosallam et al. [13]	B19	55.5	42.7	0.72	0.60	0.60	0.60	0.60
Triantafillou [14]	S1-A	21.8	8.2	1.26	1.14	1.40	1.14	1.18
	S2-A	24.1	8.2	1.26	1.26	1.26	1.26	1.26
	S3-A	21.4	8.2	1.12	1.12	1.12	1.12	1.12
	S1-45	22.3	8.2	1.20	1.16	1.18	1.16	1.25
	S3-45	22.3	8.2	1.16	1.16	1.25	1.16	1.26
Khalifa et al. [16]	BT4	162.0	90.0	1.20	0.79	0.70	0.93	0.70
	BT5	121.5	90.0	0.91	0.59	0.68	0.70	0.69
Khalifa et al. [17]	SO3-2	131.0	77.0	1.18	0.80	0.78	0.93	0.78
	SO3-3	133.5	77.0	1.06	0.84	0.84	0.84	0.84
Average				0.99	0.81	0.85	0.85	0.85
Standard Deviation				0.20	0.23	0.23	0.20	0.25
COV (%)				20.1%	28.2%	27.3%	24.1%	29.3%

Note: [1] = ACI440.2R-08 [1], [2] = *fib* Bulletin 14 [2], [3] = Chen & Teng [7], [4] = Zhang & Hsu [10], [5] = Bukhari et al [8].

$V_{n,exp}$ = ultimate shear strength of strengthened beams obtained from experiment
$V_{c,exp}$ = ultimate shear strength of control beams (without strengthening) obtained from experiment
$V_{n,STM} = V_{c,exp} + V_{frp,STM}$
$V_{frp,STM}$ = Predicted FRP shear contribution from STM

Table 5: Prediction performance on 2-sides bonded (2S) and U-wrap (U) strengthening schemes

$V_{n,exp}/V_{n,STM}$	*ACI*	*fib*	*Chen*	*Zhang*	*Buk*
2-sides bonded (2S)					
Average	1.02	0.85	0.92	0.87	0.92
COV (%)	18.6	28.9	26.0	26.5	27.9
U-wrap (U)					
Average	0.92	0.69	0.68	0.80	0.68
COV (%)	24.1	16.6	14.2	15.0	15.5

Table 6: Modes of failure prediction from STM

Reference	*Beam No*	*Experimental*	*Prediction of failure modes based on*				
		Failure modes	*ACI*[1]	*fib*[2]	*Chen*[3]	*Zhang*[4]	*Buk*[5]
Teo et al. [9]	A2	DB	DB	DB	DB	DB	DB
	A3	FC	DB	DB	DB	DB	DB
	A4	DB	DB	DB	DB	DB	DB
Zhang et al. [10]	Z4-90	DB	DB	FS	FS	FS	FS
	Z4-45	DB	DB	FS	DB	DB	DB
	Z6-90	DB	DB	FS	FS	FS	FS
	Z6-45	DB	DB	DB	DB	DB	DB
Barros et al. [11]	A10-M	S/DB	DB	FS	FS	DB	FS
	B10-M	S/DB	DB	FS	FS	DB	FS
	A12-M	S/DB	DB	FS	DB	DB	FS
	B12-M	S/DB	DB	FS	DB	DB	FS
Kim et al. [12]	CP2-1VS	S	DB	FS	DB	DB	DB
	CP2-1DS	S/DB	DB	DB	DB	DB	DB
	CP3-1VS	S/DB	DB	FS	DB	DB	DB
Mosallam et al. [13]	B19	S	DB	FS	FS	FS	FS
Triantafillou [14]	S1-A	DB	DB	FS	DB	FS	DB
	S2-A	DB	FS	FS	FS	FS	FS
	S3-A	DB	FS	FS	FS	FS	FS
	S1-45	DB	DB	FS	DB	FS	DB
	S3-45	DB	DB	FS	DB	FS	DB
Khalifa et al. [16]	BT4	DB	DB	DB	DB	DB	S
	BT5	DB	DB	DB	DB	DB	DB
Khalifa et al. [17]	SO3-2	DB	DB	DB	S	DB	S
	SO3-3	DB	DB	S	S	S	S

Note: [1] = ACI440.2R-08 [1], [2] = fib Bulletin 14 [2], [3] = Chen & Teng [7], [4] = Zhang & Hsu [10], [5] = Bukhari et al [8]. DB = FRP debonding failure, S = diagonal shear failure, FS = flexural tension failure due to steel yielding, FC = flexural compression failure.

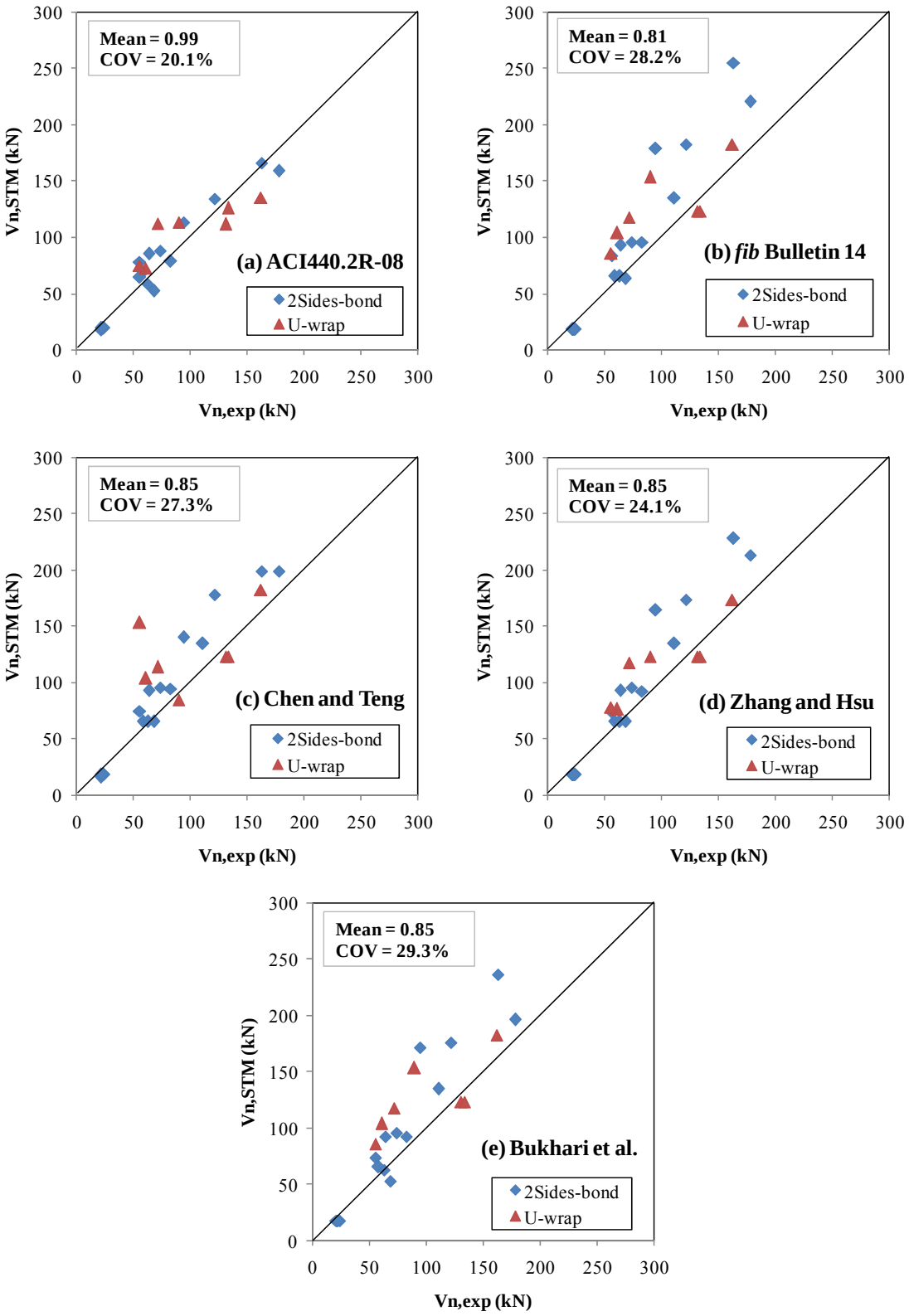

Figure 4: Comparison between $V_{n,exp}$ and $V_{n,STM}$ based on different effective FRP strains: (a) ACI440-08, (b) *fib* Bulletin 14, (c) Chen and Teng, (d) Zhang and Hsu, and (e) Bukhari et al.

ACKNOWLEDGEMENTS
The work presented in this paper was part of the second author postgraduate studies conducted at the Universiti Teknologi PETRONAS (UTP), Malaysia. Both authors would like to thank and express their gratitude and sincere appreciation to the UTP for providing financial support for the research.

REFERENCES
[1] American Concrete Institute (ACI), "Guide for the Design and Construction of Externally Bonded FRP Systems for Strengthening Concrete Structures", ACI 440.2R-08, Farmington Hills, 2008.
[2] International Federation for Structural Concrete (fib), "Externally Bonded FRP Reinforcement for RC Structures", Bulletin 14, Lausanne, Switzerland, July 2001.
[3] American Concrete Institute (ACI), "Building Code Requirements for Structural Concrete and Commentary", ACI 318-08, Farmington Hills, 2008.
[4] Ritter W., "Die Bauweise Hennebique (The Hennebique System)", Schweizerische Bauzeitung, 33, 1899, pp. 41-43, 49-52 & 59-61.
[5] Mörsch E., "Der Eisenbetonau (Concrete-steel Construction)", English translation of the third German edition, McGraw-Hill, New York, 1909, 368 pp.
[6] Schlaich J., Schäfer K. and Jennewein M., "Towards a Consistent Design of Structural Concrete", PCI Journal, 32, May-Jun 1987, pp. 74-150.
[7] Chen J. F. and Teng J. G., "Shear Capacity of FRP-strengthened RC Beams: FRP Debonding", Construction and Building Materials, 17, 2003, pp. 27-41.
[8] Bukhari I. A., Vollum R. L., Ahmad S. and Sagaseta J., "Shear Strengthening of Reinforced Concrete Beams with CFRP", Magazine of Concrete Research, Vol. 62, No. 1, 2010, pp. 65-77.
[9] Teo W., Mohd Yusuf N. H., Mbuziavo B. N. O. and Hor Y., "Evaluation of optimised truss models for FRP shear strengthened RC beams", Paper published and presented at the 18th Congress of IABSE Seoul 2012, South Korea, 19th – 21th Sept 2012.
[10] Zhang Z. C. and Hsu C. T. T., "Shear Strengthening of Reinforced Concrete Beams using Carbon-Fiber Reinforced Polymer Laminates", ASCE Journal of Composites for Construction, Vol. 9, No. 2, 2005, pp. 158-169.
[11] Barros J. A. O. and Dias S. J. E., "Near Surface Mounted CFRP Laminates for Shear Strengthening of Concrete beams", Cement & Concrete Composites, 28, 2006, pp. 277-292.
[12] Kim G., Sim J., and Oh H., "Shear Strength of Strengthened RC Beams with FRPs in Shear", Construction and Building Materials, 22, 2008, pp. 1261-1270.
[13] Mosallam A. S., and Banerjee S., "Shear Enhancement of Reinforced Concrete Beams Strengthened with FRP Composite Laminates", Composites: Part B, 38, 2007, pp. 781-793.
[14] Triantafillou T. C., "Shear Strengthening of Reinforced Concrete Beams using Epoxy-Bonbed FRP Composites", ACI Structural Journal, Vol. 95, No. 2, March-April 1998, pp. 107-115.
[15] Triantafillou T. C. and Antonopoulos C. P., "Design of Concrete Flexural Members Strengthened in Shear with FRP", ASCE Journal of Composites for Construction, Vol. 4, No. 4, Nov. 2000, pp. 198-205.
[16] Khalifa A. and Nanni A., "Improving Shear Capacity of Existing RC T-section Beams Using CFRP Composites", Cement & Concrete Composites, 22, 2000, pp. 165-174.
[17] Khalifa A. and Nanni A., "Rehabilitation of Rectangular Simply Supported RC Beams with Shear Deficiencies Using CFRP Composites", Construction and Building Materials, 16, 2002, pp. 135-146.
[18] Khalifa A., Gold W. J., Nanni A. and Aziz A., "Contribution of Externally Bonded FRP to Shear Capacity of RC Flexural Members", ASCE Journal of Composites for Construction, Vol. 2, No. 4, Nov. 1998, pp. 195-202.
[19] Marti P., "Basic Tools of Reinforced Concrete Beam Design", ACI Journal, Vol. 82, Jan-Feb 1985, pp. 46-56.